3-15-2005

# Role of Hydrogen Bonds in the Fast Dynamics of Binary Glasses of Trehalose and Glycerol: a Molecular Dynamics Simulation Study

Taner E. Dirama

Gustavo A. Carri
*University of Akron Main Campus*, gac@uakron.edu

Alexei P. Sokolov

# Role of hydrogen bonds in the fast dynamics of binary glasses of trehalose and glycerol: A molecular dynamics simulation study

Taner E. Dirama, Gustavo A. Carri,[a] and Alexei P. Sokolov
*Department of Polymer Science, The University of Akron, Akron, Ohio 44325*

(Received 9 November 2004; accepted 20 January 2005; published online 17 March 2005)

Trehalose-glycerol mixtures are known to be effective in the long time preservation of proteins. However, the microscopic mechanism of their effective preservation abilities remains unclear. In this article we present a molecular dynamics simulation study of the short time, less than 1 ns, dynamics of four trehalose-glycerol mixtures at temperatures below the glass transition temperature. We found that a mixture of 5% glycerol and 95% trehalose has the most suppressed short time dynamics (fast dynamics). This result agrees with the experimental analysis of the mean-square displacement of the hydrogen atoms, as measured via neutron scattering, and correlates with the experimentally observed enhancement of the stability of some enzymes at this particular concentration. Our microscopic analysis suggests that the formation of a robust intermolecular hydrogen bonding network is most effective at this concentration and is the main mechanism for the suppression of the fast dynamics. © *2005 American Institute of Physics*. [DOI: 10.1063/1.1870872]

## I. INTRODUCTION

The ability of carbohydrate glasses to preserve biomolecules has been well documented for two decades now.[1–3] However, the molecular mechanisms that govern this phenomenon are not fully understood yet. Some researchers have attributed the protective effect of carbohydrates on freeze-dried proteins to their ability to form hydrogen bonds to the protein, thus serving as water substitutes.[2,3] Other researchers have pointed out the importance of glass formation in the preservation capabilities of carbohydrate glasses.[4,5] This is a consequence of the fact that protein stability often correlates with the glass transition temperature $T_g$ of the media that hosts the protein.[4,6–8] Yet, there are reports that contradict with this argument.[9–11]

One of the most promising carbohydrates is trehalose ($\alpha$-D-glucopyranosyl $\alpha$-D-glucopyranoside), Fig. 1. This sugar is found in many organisms that suffer dehydration stresses. Trehalose, with four hydroxyl sites in each ring, is capable of making hydrogen bonds with the polar and charged groups of proteins that are normally hydrated. This results in the creation of an environment that is similar, in terms of the local dynamics of the protein, to the one seen by the protein in aqueous solutions.[4,12–16] On the other hand, Magazu and co-workers have suggested that the protective ability of trehalose on biological structures can be attributed to the fragile character of this glass former.[17] A small thermal excitation in fragile glasses leads to a reorganization in the structure while strong glasses show a resistance to structural changes.[18] They speculated that this sensitivity of trehalose to changes in temperature could enable the molecule to rearrange its conformation, mainly by rotation around the glycosidic oxygen, so that the molecule will form hydrogen bonds with the rough surface of the protein.

The growing recognition of the importance of trehalose in cryoprotection and lyoprotection of proteins motivated the experimental[19,20] and computational[21–24] study of many aspects of trehalose including its glass transition behavior, hydration, thermophysical properties, and conformational changes. In this area, molecular simulations are of significant value since they can contribute to the understanding of the molecular mechanisms that take place in biopreservation.

As stated previously, protein stability is often correlated with $T_g$ of the glassy host.[4,6–8] However, Cicerone *et al.*[11,25] have recently reported that the addition of a small amount of diluent reduces $T_g$ (i.e., reduces the viscosity) while improving the stability of the protein in the glassy host. Therefore, the work by Cicerone and co-workers contradicts the correlation between protein stability and $T_g$ of the glassy host, suggesting that the viscosity of the medium is not the only variable controlling protein stability. In addition, all the systems studied by this group were glassy. Thus, the physical origin of the improved stability of the biomolecule is dynamic in nature (slower denaturation) and not thermodynamic (increased stability of the folded state). Specifically, Cicerone and co-workers probed the stability of two enzymes (horseradish peroxide and yeast alcohol dehydrogenase) embedded in glycerol-trehalose glasses with various compositions by measuring the deactivation times of the enzymes at various temperatures.[11] The deactivation times showed a maximum at 5% glycerol concentration in the trehalose matrix. Later, Cicerone and Soles reported a neutron scattering study where they observed the suppression of the short time local dynamics at the same glycerol concentration suggesting that there is a correlation between the preservation of enzymes and the suppression of short time local dynamics.[25] This correlation between short time scale dynamics (suppression of the fast dynamics) and the long time scale dynamics (preservation of the enzymes) might be difficult to accept because of the large difference in time scales

[a]Author to whom correspondence should be addressed. Electronic mail: gac@uakron.edu

 

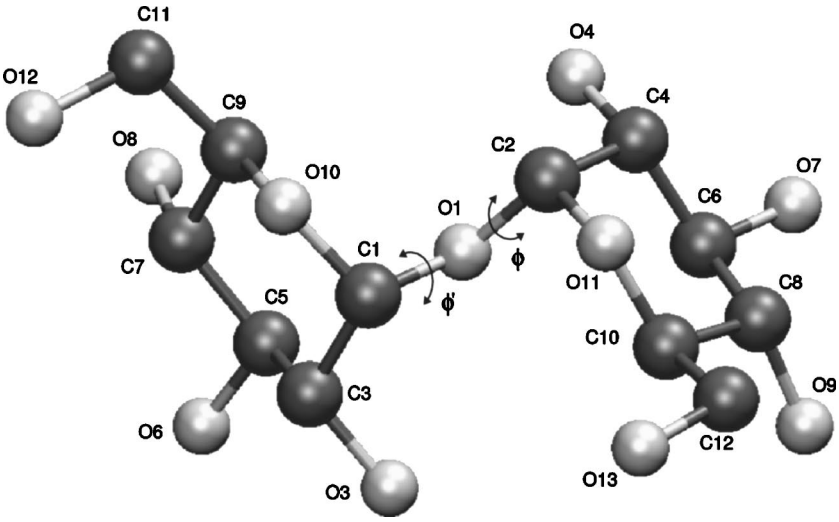


FIG. 1. Trehalose ($\alpha$-D-glucopyranosyl $\alpha$-D-glucopyranoside). Hydrogen atoms are not shown to maintain clarity. Glycosidic dihedral angles $\phi$ and $\phi'$ are also shown.

(15 decades approximately). However, there are indications in the field of simple glass formers that suggest a connection between the slow and fast dynamics of glassy systems:[26] a stronger suppression of the fast dynamics correlates with a weaker temperature dependence of the viscosity (i.e., less fragile system). Based on the results of Ref. 11, the authors of Ref. 27 speculated that the fragility of the solvent is another important parameter for protein preservation. This speculation explains the earlier observation that sucrose provides better preservation than raffinose, despite its lower $T_g$. Sucrose appears to be less fragile than raffinose.

The correlation between the preservation of enzymes and the suppression of short time local dynamics suggests two conclusions. First, an efficient formulation should suppress the local and short time dynamics of a protein which is a precursor to protein denaturation and, second, the dynamics of the protein follows the one of the solvent. The latter suggestion has been extensively studied and documented by Frauenfelder and co-workers.[28] In addition, the slaving of the protein dynamics has also been reported by Paciaroni *et al.*[29] and more recently by Caliskan *et al.*[27] who showed that in lysozyme-trehalose or glycerol solutions the protein dynamics follows *that of* the solvents.

The findings by Cicerone and Soles[25] motivated us to investigate the same mixtures with the purpose of understanding the molecular origins of this unexpected behavior. Therefore, we investigated the short time dynamics of a few trehalose/glycerol mixtures at temperatures below $T_g$ using molecular dynamics simulations. We adopted the general amber force field (GAFF) (Ref. 30) developed for general organic molecules in a fully flexible all-atom model. The mean-square displacement $\langle u^2 \rangle$ of *the hydrogens in trehalose* was found to change with the addition of glycerol and, moreover, has a minimum at 5% glycerol concentration, in good agreement with the experimental observations of Cicerone and Soles.[25] Furthermore, our study showed the formation of a more robust hydrogen bonded network at this particular concentration and, moreover, evidence that this enhancement of hydrogen bonding contributes to the suppression of the fast dynamics.

## II. SIMULATION PROTOCOL

The AMBER molecular dynamics package[31] with GAFF (Ref. 30) was used in this study. The structures of trehalose,[32] Fig. 1, and glycerol,[33] Fig. 2, molecules in their crystalline states were optimized and their electrostatic potentials on atom surfaces were calculated using GAUSSIAN 03.[34] The Gaussian calculation was done using (ground state) Hartree–Fock method with 6-31G basis set. Point charges on the atomic nuclei were then fitted by restrained electrostatic potential (RESP). The simulation boxes were created using optimized structures of trehalose and glycerol molecules with glycerol compositions (by weight) $\phi_{glycerol}=0$, 0.05, 0.10, 0.15, and 1. The resulting boxes contained 20 000 atoms approximately.

Rectangular parallelepiped periodic boundary conditions were used. Long-range electrostatic interactions were calculated using the particle-mesh Ewald method, while van der Waals (vdW) interactions were calculated using the 6-12 Lennard-Jones potential. The cutoff distance for nonbonded van der Walls interactions was set to 8 Å. However, in the case of electrostatic interactions this cutoff is used for the evaluation of Ewald's standard direct sum; corrections are taken into account via the reciprocal sum. The hydrogen bonds in this all-atom potential function are represented by a balance between electrostatic and van der Waals interactions. The equations of motion were integrated using the leap-frog

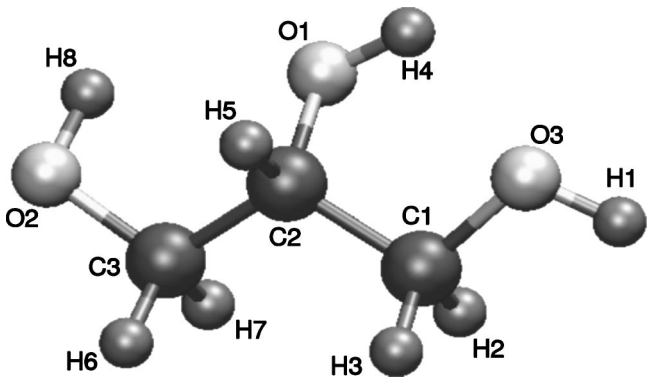


FIG. 2. Glycerol (1,2,3-propantriol).

Verlet algorithm with a step size of 1 fs. The simulation boxes were equilibrated in the *N-V-T* ensemble at 500 K for 100 ps followed by a 200 ps *N-P-T* simulation to reach the equilibrium density. In the *N-P-T* simulation the pressure was set to 0.1 MPa. Afterward, each box was annealed to 300 K at a cooling rate of 0.1 K/ps followed by equilibration in the *N-P-T* ensemble at 300 K for 1 ns. Similarly, for 250 and 200 K the simulation box was annealed to these temperatures at the same rate of 0.1 K/ps and equilibrated for 1 ns in the *N-P-T* ensemble. Data collection run in the *N-P-T* ensemble was performed for 1 ns and coordinate sets were saved for every 0.1 ps intervals for subsequent analysis. Constant temperature and pressure were satisfied by a weak coupling algorithm.[35]

We estimated the glass transition temperature of pure trehalose and its mixtures by computing the density of the system at different temperatures. For these estimates, the simulation boxes consisted of 46 trehalose and the corresponding number of glycerol molecules to match the desired compositions. Consecutive *N-P-T* simulations after equilibration at 600 K were carried out. The simulation boxes were cooled at a rate of 0.2 K/ps between each consecutive temperature where data were collected for 200 ps keeping the temperature constant.

## III. RESULTS

The first property of interest is the density of the pure components and their mixtures. The simulation value for the density of glycerol at 300 K is 1.25 g/cm$^3$ which agrees very well with the experimental value of 1.254 g/cm$^3$.[36] For trehalose, the simulation yields 1.47 g/cm$^3$, while the experimental value is 1.53 g/cm$^3$.[37] An earlier simulation study by Conrad and de Pablo[24] has estimated the density of trehalose at 300 K to be 1.47 g/cm$^3$, in good quantitative agreement with our estimate.

Figure 3(a) shows the density of the mixtures for various compositions at 300 K. The standard deviations of the density data are smaller than 1% in all cases. Since the error bars are of the same size of the symbols, they are not shown in the plot. From this figure it is clear that the addition of 5% (by weight) of glycerol to pure trehalose slightly increases the density of the system. Further addition of glycerol decreases the density of the mixture, as it is expected for a diluent. Therefore, the density of the mixture shows a nonmonotonic change with glycerol concentration. The same behavior was also observed at 200 and 250 K (not shown).

Another quantity of interest is $\langle u^2\rangle(t)$ which is defined as the mean-square displacement of *the hydrogen atoms in trehalose* at time $t$. For the purpose of illustration, we show $\langle u^2\rangle(t)$ for the case of pure trehalose in Fig. 4. Similar curves were obtained for all the mixtures. The figure clearly shows a plateau for all the three temperatures studied. These plateaus last for different periods of time. For example, at 200 and 250 K the plateau lasts for 800 ps, whereas at 300 K $\langle u^2\rangle(t)$ starts to increase after 200 ps. Averaging $\langle u^2\rangle(t)$ over 1 ns ($=\langle u^2\rangle$) gives the mean-square displacement which is plotted as a function of glycerol concentration at 300 K in Fig. 3(b). The stronger suppression of the dynamics at 5% glycerol concentration is clearly showed. $\langle u^2\rangle$ was used to characterize the short time dynamics of trehalose in the study by Cicerone and Soles.[25] The agreement between our calculations for $\langle u^2\rangle$ and the experimental ones, shown in Table I, is reasonable implying that our simulation study can provide accurate predictions for dynamic quantities. Also note that both experimental and simulation results for $\langle u^2\rangle$ show a minimum at $\phi_{glycerol}=0.05$ for all three temperatures.

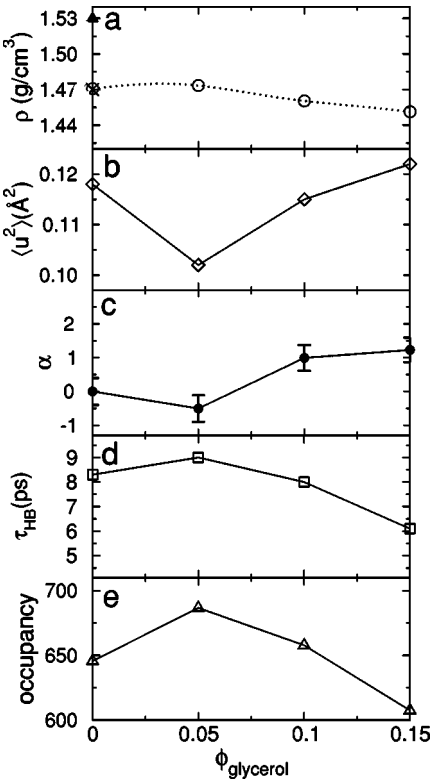


FIG. 3. (a) Density of trehalose-glycerol mixtures at 300 K (○) from MD simulations (this work), (×) Conrad and de Pablo (Ref. 24), and (△) experimental value (Ref. 37); (b) composition dependence of the mean-square displacement at 300 K; (c) $\alpha$ vs $\phi_{glycerol}$; (d) effect of composition on the lifetime of the hydrogen bonds $\tau_{HB}$; and (e) on the occupancy of hydrogen bonds at 300 K.

Another property of the system is its $T_g$. We estimated $T_g$ using a method very similar to the one employed in Ref. 24 where the density is plotted as a function of temperature and $T_g$ is the temperature where the slope shows a discontinuity. Figure 5 shows the case of 5% glycerol–95% trehalose mixture. A clear change in the slope is observed at 480 K. In all

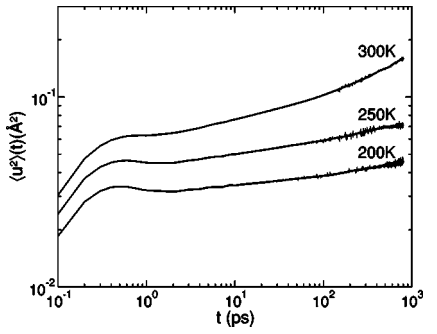


FIG. 4. Mean-square displacement (in Å$^2$) as a function of time (in ps) for trehalose at 200, 250, and 300 K.

TABLE I. Mean-square displacement (in $Å^2$) at various temperatures and estimates for the glass transition temperatures of pure trehalose and mixtures. Experimental data are from Ref. 25.

| $\phi_{glycerol}$ | $T$ (K) | 200 | 250 | 300 | $T_g$ (K) |
|---|---|---|---|---|---|
| 0.00 | Experimental | 0.049 | 0.069 | 0.104 | 391 |
| | Simulation | 0.041 | 0.063 | 0.118 | 456 |
| 0.05 | Experimental | 0.025 | 0.040 | 0.070 | 370 |
| | Simulation | 0.036 | 0.059 | 0.102 | 480 |
| 0.10 | Experimental | 0.045 | 0.070 | 0.104 | 341 |
| | Simulation | 0.039 | 0.065 | 0.115 | 420 |
| 0.15 | Experimental | 0.045 | 0.075 | 0.120 | 331 |
| | Simulation | 0.041 | 0.066 | 0.122 | 427 |

the cases we studied, the values of $T_g$ obtained from simulations are significantly higher than the experimental ones (Table I). Also, our estimate of $T_g$ for pure trehalose is somewhat better than the one reported in Ref. 24. This might be due to the gradual cooling between the temperatures where the measurements were done as opposed to starting the simulation at the next temperature from the last configuration at the previous temperature. It is worth observing the nonmonotonic dependence of $T_g$ on glycerol concentration displayed by our simulation study. This behavior disagrees with the experimental observations of Cicerone and Soles.[25] The physical origin of the different behaviors will be clarified in the following section using the concept of fragility.

The aforementioned results show that the 5% glycerol–95% trehalose mixture is the most dense system, the one with the highest $T_g$ (in our simulation study) and smallest mean-square displacement. All these observations could be rationalized if the attractive interactions between the atoms were the strongest ones for this particular system. In other words, this mixture should display the highest cohesive energy density. This line of reasoning led us to compute the van der Waals energy per atom for each of the mixtures. Figure 3(c) shows the effect of glycerol concentration on the parameter $\alpha$ at 300 K. $\alpha$ is defined as $(e_{vdW,0}-e_{vdW,\phi})/e_{vdW,0} \times 100$ representing the percentile deviation of the vdW energies from that of pure trehalose, where $e_{vdW,0}$ and $e_{vdW,\phi}$ are the vdW energies per atom for pure trehalose and a trehalose-glycerol mixture with a concentration of glycerol equal to $\phi$, respectively. For all the temperatures studied (200 and 250 K not shown here), the 5% glycerol–95% trehalose mixture has the most negative vdW energies. In other words, for this particular composition the attractive force between atoms is the strongest one. Knowing that hydrogen bonding is taken into account in the vdW term of the force field, one can speculate that this minimum in the vdW energy may be a consequence of a peculiar hydrogen bonding behavior of this highly hydrogen bonding capable mixture. We evaluated the hydrogen bonding behavior of the glycerol-trehalose system using the geometric criterion which is based on the distance between the donor and the acceptor oxygens, and the angle formed by the donor oxygen, the acceptor hydrogen, and the acceptor oxygen.[38] The cutoff distance between oxygen atoms was set to 3.4 Å which is about the location of the minimum after the first peak of the radial distribution function; the cutoff for the angle was set to 120°. The occupancy and the mean hydrogen bonding lifetime ($\tau_{HB}$) of the intermolecular hydrogen bonds were calculated over a 1 ns trajectory. The occupancy is defined as the average number of simulation steps during which a hydrogen bond existed where the averaging is done over all hydrogen bonds (i.e., we look at an individual atom pair, trace it to see how many times there is a formation of a hydrogen bonding interaction during the simulation, and then we average over all hydrogen bonding pairs of atoms); $\tau_{HB}$ is the occupancy multiplied by the time step (0.1 ps) and divided by the number of times that the hydrogen bond is broken. The average results over all hydrogen bonds as function of composition and temperature were obtained after applying cutoffs for occupancy and $\tau_{HB}$. This was done with the purpose of removing the effects of those hydrogen bonds that form and break very quickly, thus not affecting the dynamics significantly. Explicitly, the averages were computed using those hydrogen bonds that live longer than 1 ps and form more than 3% of the production run. The hydrogen bonds were classified with respect to the pairs of molecules that form the bond (Table II). It is important to observe that the 5% glycerol–95% trehalose mixture always has the longest lifetimes and highest occupancies. Figures 3(d) and 3(e) show the lifetimes and occupancies of hydrogen bonds as a function of glycerol concentration at 300 K. Note that the changes in these quan-

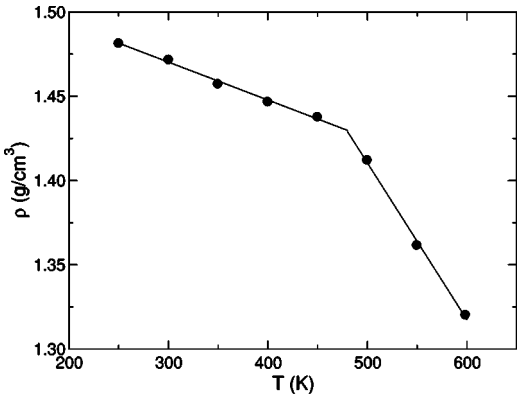


FIG. 5. Plot of the density ($\rho$ in g/cm$^3$) as a function of temperature (in K) for the 5% glycerol–95% trehalose mixture.

TABLE II. Hydrogen bond lifetime $\tau_{HB}$ (in ps) and occupancy $n$ for pure trehalose and mixtures at various temperatures.

| | | 0.00 | | 0.05 | | 0.10 | | 0.15 | |
|---|---|---|---|---|---|---|---|---|---|
| Molecule Pairs | $\phi_{glycerol}$ $T$ (K) | $\tau_{HB}$ | $n$ | $\tau_{HB}$ | $n$ | $\tau_{HB}$ | $n$ | $\tau_{HB}$ | $n$ |
| | 200 | 155.4 | 906.5 | 173.7 | 930.3 | 156.2 | 920.3 | 138.6 | 885.3 |
| Any | 250 | 40.6 | 834.1 | 53.1 | 835.6 | 43.1 | 817.3 | 36.1 | 789.5 |
| | 300 | 8.3 | 645.6 | 9.0 | 686.7 | 8.0 | 657.8 | 6.1 | 607.5 |
| | 200 | 155.4 | 906.5 | 176.2 | 927.7 | 167.6 | 915.2 | 159.5 | 896.7 |
| Tre-Tre | 250 | 40.6 | 834.1 | 53.3 | 843.6 | 46.1 | 837.2 | 45.9 | 829.6 |
| | 300 | 8.3 | 645.6 | 9.7 | 702.5 | 8.7 | 704.5 | 7.3 | 656.8 |
| | 200 | ⋯ | ⋯ | 165.8 | 950.9 | 127.5 | 935.8 | 104.6 | 870.7 |
| Tre-Glc | 250 | ⋯ | ⋯ | 54.7 | 803.4 | 36.1 | 769.5 | 22.8 | 741.9 |
| | 300 | ⋯ | ⋯ | 5.7 | 611.5 | 6.5 | 553.9 | 4.3 | 542.5 |

tities are significant. We also investigated the occurrence of intramolecular hydrogen bonding in trehalose molecules and a similar trend was observed.

The formation of intramolecular hydrogen bonds has important implications for the conformation of trehalose. Indeed, it has been reported that trehalose can fold onto a protein and substitute water molecules during drying by rearranging its conformation.[17] The conformation of trehalose is determined by the glycosidic dihedral angles: $\phi$ and $\phi'$ (Fig. 1). Figure 6 shows the values of these two dihedral angles *averaged* over all the trehalose molecules present in the simulation box for *each* of the 10 000 snapshots taken during the 1 ns molecular dynamics (MD) trajectory for each mixture. Each point showed in Fig. 6 has an error of 20° (not shown). The collection of the average values of these two dihedral angles for the mixtures appears to deviate from the values found in the crystalline state by a few degrees only. Likewise, the conformations of trehalose in the different mixtures are very similar. It is apparent that the addition of glycerol into the trehalose matrix does not have a significant effect on the conformation of the molecules. In addition, Fig. 6 indicates that the conformation of trehalose at temperatures below $T_g$ is almost locked around a minimum that is close to its conformation in the crystalline state.

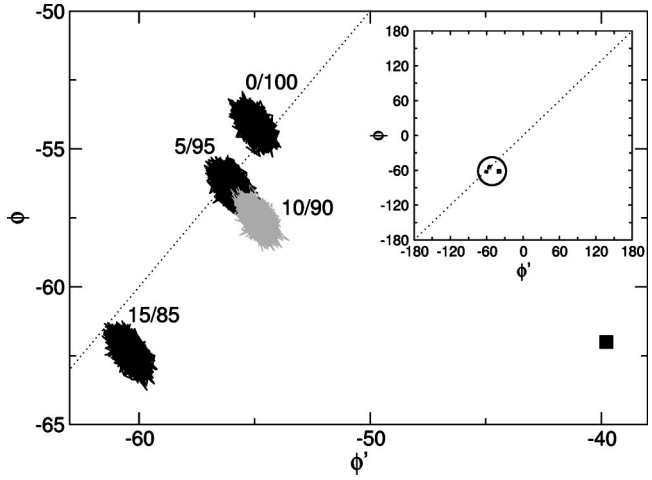


FIG. 6. Average dihedral angles of glycosidic oxygens at 200 K for various compositions throughout the 1 ns MD trajectory. $\phi$ and $\phi'$ are the dihedral angles formed by C1, O1, C2, HC2 and C2, O1, C1, HC1, respectively. ■ indicates the values of these dihedral angles for pure trehalose in the crystalline state. The inset shows the same data plotted over whole space of dihedral angles. The dotted line is the diagonal line.

## IV. DISCUSSION

Our study predicts a nonmonotonic dependence of $T_g$ on glycerol concentration. The addition of glycerol increases the value of $T_g$ initially, while further addition of glycerol decreases $T_g$ (Table I). However, the experimental (calorimetric) $T_g$ decreases monotonically with increasing glycerol concentration.[25] The origin of this apparent discrepancy is in the different time scales involved in calorimetric measurements (100 s approximately) and current molecular dynamics simulations (typical cooling rates are of the order of a Kelvin degree per picosecond). Consequently, regardless of how slow the cooling rate in the simulation is, it will always be substantially faster than the ones currently achievable in real experimental studies. Thus, the estimate for $T_g$ arising from a simulation will always be higher than the experimental one.

The different values of $T_g$ for the times scales mentioned in the previous paragraph led us to study the fragility of the mixtures. For this purpose, we employ the ratio $32.2R/[1-T_g(100\ \mathrm{s})/T_g(10^{-12}\ \mathrm{s})]$ which is an *approximate estimate* of the fragility of the system defined as the ratio between the activation energy $\Delta E$ and $T_g$; $R$ is the ideal gas constant (in kJ/mol K) and $T_g(100\ \mathrm{s})/T_g(10^{-12}\ \mathrm{s})$ is the ratio of the experimental to the simulation $T_g$. This estimate is derived from the standard definition of fragility $F$ (Ref. 26)

$$F = \frac{\Delta E}{T_g} = \frac{R}{T_g}\left.\frac{d\ln(\tau)}{d\left(\frac{1}{T_g}\right)}\right|_{T=T_g} = \frac{2.305R}{T_g}\left.\frac{d\ln(\tau)}{d\left(\frac{1}{T_g}\right)}\right|_{T=T_g}, \quad (1)$$

where we approximate the derivative by finite differences as follows:

$$\left.\frac{d\ln(\tau)}{d\left(\frac{1}{T_g}\right)}\right|_{T=T_g} \approx \frac{\ln(100\ \mathrm{s}) - \ln(10^{-12}\ \mathrm{s})}{\frac{1}{T_g(100\ \mathrm{s})} - \frac{1}{T_g(10^{-12}\ \mathrm{s})}}. \quad (2)$$

Observe that our estimate for the fragility will always be lower than the experimental value. Large values indicate more fragile glasses while smaller numbers imply stronger glasses. The results for the fragilities are 1.88, 1.17, 1.42, 1.19, and 0.81 kJ/mol K for pure trehalose, 5% glycerol–95% trehalose mixture, 10% glycerol–90% trehalose mixture, 15% glycerol–85% trehalose mixture, and pure glycerol glasses, respectively. The literature values for the fragility of glycerol and trehalose are 1.11 kJ/mol K (Ref. 26) and 3.15 kJ/mol K,[39] respectively. These experimental results imply that our estimates and the experimental values of the fragility are in reasonable qualitative agreement. The first conclusion arising from the values of the fragility is that glycerol is a stronger glass former than trehalose, which is known to be a fragile glass.[17] Moreover, the addition of only 5% glycerol to trehalose decreases its fragility significantly. Beyond this point, fragility first increases and then decreases with the further addition of glycerol. Clearly, glycerol changes the fragility of the sugar in a nonmonotonic manner. Sokolov *et al.*[26] have shown that fast conformational fluctuations at temperatures below $T_g$ are more suppressed in strong glasses than in fragile glasses. Thus, the fast dynamics of trehalose is more suppressed at 5% glycerol concentration than for pure trehalose which agrees with our analysis of $\langle u^2 \rangle$ presented below. Based on these ideas, Caliskan *et al.*[27] speculated that the stronger solvents may provide better preservation. Our simulation studies on glycerol-trehalose mixtures support this idea; stronger glasses may provide a better suppression of the fast dynamics in proteins.

The suppression of the fast dynamics is clearly observed in $\langle u^2 \rangle$. A quantitative comparison of $\langle u^2 \rangle$ at different compositions exhibits a minimum at 5% glycerol concentration for all the three temperatures [Table I and Fig. 3(b)] indicating that the dynamics of trehalose is suppressed by the addition of a small amount of glycerol. The decrease of $\langle u^2 \rangle$ predicted by our simulations is not as pronounced as the one observed experimentally. However, the experimentally observed trend in glycerol-trehalose mixtures is definitely captured by our simulations. The quantitative differences between the experimental and simulation results for the 5% glycerol–95% trehalose mixture can have many origins. In our view, one of the main reasons is the equilibration time accessible to MD simulations which is substantially shorter than the experimental one. Considering that the simulations of all the mixtures are performed below $T_g$, it is highly probable that the simulation boxes may be further away from their thermodynamic equilibrium states than the actual samples. Another possible reason was discussed in Ref. 25 where the authors mentioned that for fully hydrogenated glasses, as is the case of our simulation, the magnitude of the maximum suppression at 5% glycerol concentration is slightly less than the one they measured using *deuterated* glycerol.

The initial increase in density with the addition of glycerol suggests that the strength of the attractive interactions is changed. This increase in the attractive interactions should also make the motion of the atoms more difficult, thus suppressing the fast dynamics. We studied the interactions present in our simulation and found that for the mixture made of 5% glycerol–95% trehalose the attractions between atoms are the strongest. We determined that the origin of this enhancement was due to a change in the hydrogen bonding network of the system which appears in the average lifetime of the hydrogen bonds $\tau_{HB}$ and the occupancy [Table II and Figs. 3(d) and 3(e)]. When all hydrogen bonds are considered both $\tau_{HB}$ and occupancy reach a maximum at 5% glycerol concentration. The same trend holds for the hydrogen bonds formed between trehalose molecules and, between trehalose and glycerol molecules. This result shows that at 5% glycerol concentration hydrogen bond formation is relatively more frequent than for the other compositions and, moreover, the average lifetime is longer. Consequently, the molecular origin of the stronger attractions between atoms for the 5% glycerol–95% trehalose mixture is the existence of a more robust hydrogen bonding network.

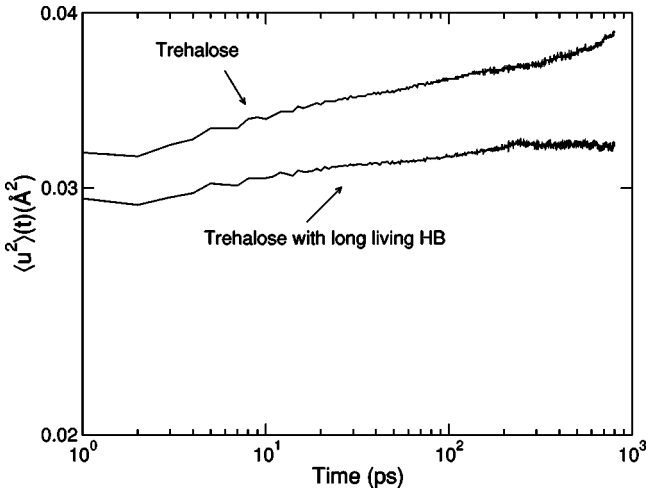


FIG. 7. Comparison of the mean-square displacement (in Å$^2$) between all trehalose molecules and 25% of those that form long-living hydrogen bonds.

We explored the correlation between the suppression of the dynamics and the formation of hydrogen bonds by studying the case of $\phi_{glycerol}=0.05$ and comparing $\langle u^2 \rangle$ of *all* trehalose molecules with $\langle u^2 \rangle$ for those trehalose molecules that form the longest living hydrogen bonds and have the highest occupancy (Fig. 7). We found that at 200 K the $\langle u^2 \rangle$ obtained for all trehalose molecules and for those forming long-living hydrogen bonds were 0.036 Å$^2$ and 0.031 Å$^2$, respectively. Similar results were obtained at 250 and 300 K. This result shows a direct correlation between hydrogen bonding and $\langle u^2 \rangle$, while it supports the idea that the enhanced hydrogen bonding observed at 5% glycerol concentration is the cause of suppression of the short time dynamics.

We also studied the existence of intramolecular hydrogen bonds in trehalose molecules. Our study showed that the occurrence of intramolecular hydrogen bonds is very rare when compared to the formation of intermolecular hydrogen bonds and their lifetimes are two orders of magnitude

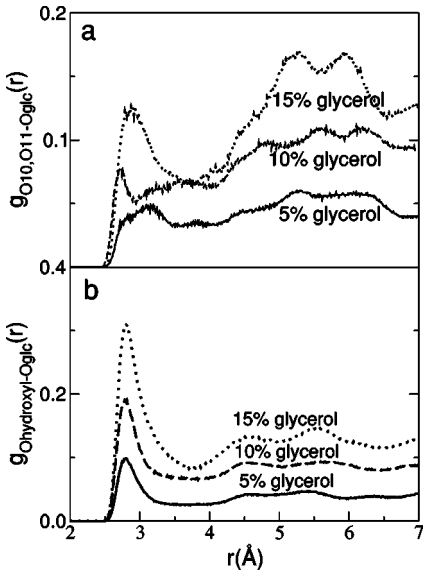


FIG. 8. Radial distribution function between (a) all O10 and O11 oxygens in trehalose and all the oxygen atoms in glycerol, (b) all hydroxyl oxygens in trehalose and all the oxygen atoms in glycerol for various compositions and at 200 K.

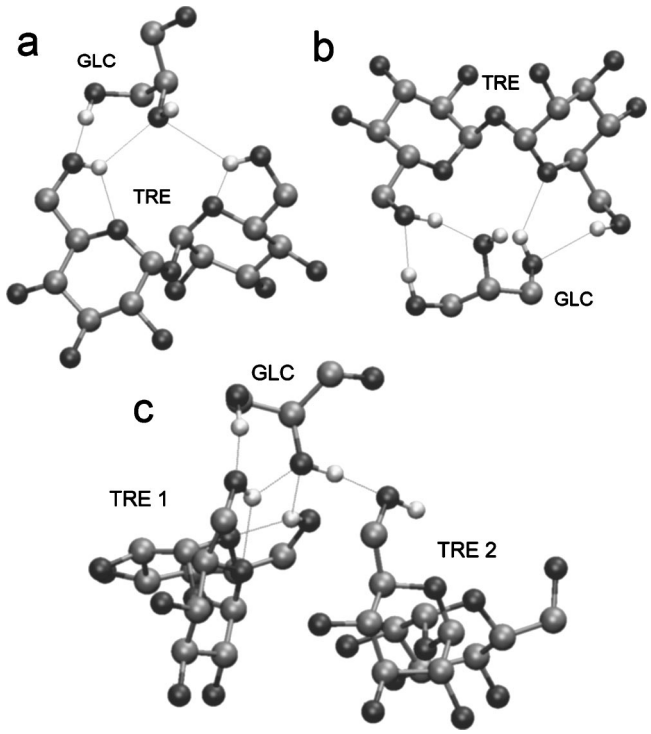


FIG. 9. Snapshots illustrating glycerol and trehalose hydrogen bond formation from MD simulations of the 5% glycerol–95% trehalose mixture. Snapshots were created using the VMD molecular visualization program (Ref. 40).

shorter. Therefore, the effects of intramolecular hydrogen bonding on the dynamics of the system are not expected to be significant.

Another property of interest is the conformation of trehalose. It has been proposed[19] that the fragile nature of trehalose might enable these molecules to change their conformations relatively easily and form hydrogen bonds with the rough surfaces of proteins by replacing water molecules. However, our MD simulations showed no significant change in the average conformations of trehalose molecules with respect to the one in the crystalline state.

Although our simulation study suggests that the molecular origin of the suppression of the fast dynamics is the formation of a robust hydrogen bonding network, it does not specify how glycerol is improving the hydrogen bonding capabilities of trehalose and why the optimum glycerol concentration is 5%. In order to clarify this point, we have calculated several radial distribution functions between different groups of oxygen atoms in trehalose and all the oxygen atoms in glycerol at different temperatures. We only show the most relevant results for a temperature of 200 K but similar conclusions were obtained for 250 and 300 K. First, it was observed that the glycosidic oxygen (O1) does not form hydrogen bonds with glycerol, as expected due to steric hindrance. The radial distribution function involving oxygens O10 and O11 is showed in Fig. 8(a). This plot shows a peak around 3 Å for all compositions indicating that O10 and O11 do form hydrogen bonds with glycerol and that this contribution is not negligible. The number of these bonds is smaller than for the hydroxyl groups due to steric hindrance, as we discuss below. However, their effects on the fast dynamics should be significant because if a hydrogen bond is formed, it is likely that the other hydroxyl groups in glycerol will form a hydrogen bond with the other ring. Such glycerol bridges, which were observed in our simulations as shown in Fig. 9(a), would constrain the motion of the whole trehalose molecule, thus suppressing its dynamics. Figure 8(a) also shows other peaks at distances close to 6 Å which suggest the presence of glycerol close to the edges of the rings. Figure 8(b) shows the radial distribution function for the oxygens in the hydroxyl groups of trehalose and all the oxygens in glycerol. The peaks present at a distance close to 3 Å clearly show that glycerol is concentrated mainly around the hydroxyl groups at a distance where the formation of hydrogen bonds is possible. We can envision various possible scenarios. First, glycerol might be forming two or three hydrogen bonds with the hydroxyl groups on one of the rings restraining the motion of those hydrogen atoms. In addition, it would also reduce the motion of the whole ring because it increases its bulkiness, thus suppressing the dynamics of all the hydrogens in that ring as illustrated in the snapshot showed in Fig. 9(b). Second, neighboring trehalose molecules might be better correlated by hydrogen bonds formed through glycerol bridges than by hydrogen bonds between the hydroxyl groups in the rings. This scenario can be rationalized by the fact that glycerol could form hydrogen bonds with two hydroxyl groups on one trehalose molecule and one on another trehalose molecule as shown by the snapshot depicted in Fig. 9(c). Clearly, the simultaneous formation of three hydrogen bonds would lead to a stronger correlation between the molecules which, in turn, should suppress their dynamics. The above scenarios, which were exemplified by the instances taken from the simulations, may explain how glycerol enhances the hydrogen bonding capability of trehalose.

## V. CONCLUSIONS

Cicerone and co-workers have recently suggested a correlation between the preservation of enzymes in glassy hosts and the suppression of the short time local dynamics of the glass. In particular they reported that the addition of glycerol to a glassy trehalose matrix enhances the stability of the enzymes while reducing the glass transition temperature of the host and suppressing the dynamics of the trehalose molecules. In this article we have shown that the molecular origins of this complex behavior can be found in the hydrogen bonding network of the glassy host. Indeed, the initial addition of glycerol to the trehalose matrix forms a robust hydrogen bonding network characterized by higher occupancies and longer lifetimes. Further addition of glycerol leads to a situation where the liquid nature of glycerol starts to control the physical properties of the mixture and, consequently, the hydrogen bonding network becomes weaker. Analysis of the data also showed that glycerol has a tendency to form hydrogen bonds with the hydroxyl groups of trehalose. This leads to the suppression of the dynamics of trehalose. In summary, our study has shown that the stronger hydrogen bonding network that occurs at 5% glycerol concentration has important implications in many equilibrium and dynamic properties such as density, glass transition temperature, fragility, and atomic mean-square displacement.

## ACKNOWLEDGMENTS

The authors thank Dr. Cicerone for providing them with a preliminary copy of Ref. 25 and for useful discussions. G.A.C. also acknowledges Dr. Angel Garcia for bringing Ref. 28 to his attention during his visit to Los Alamos National Laboratory. This material was based upon work partially supported by The National Science Foundation under Grant Nos. CHE-0132278 and DMR-0315388. Also, acknowledgment is made to the Donors of The Petroleum Research Fund, administered by the American Chemical Society, for partial support of this research (PRF No. 37051-G7) and The Ohio Board of Regents, Action Fund (Grant No. R566).

[1] R. Mouradian, C. Womersley, L. M. Crowe, and J. H. Crowe, Biochim. Biophys. Acta **778**, 614 (1984).
[2] J. F. Carpenter and J. H. Crowe, Biochemistry **28**, 3916 (1989).
[3] J. F. Carpenter, S. J. Prestrelski, and T. Arakawa, Arch. Biochem. Biophys. **303**, 456 (1993).
[4] J. L. Green and C. A. Angell, J. Phys. Chem. **93**, 2880 (1989).
[5] C. A. Angell, in *Hydrogen-Bonded Liquids*, edited by J. C. Dore and J. Teixeira (Kluwer, Dordrecht, 1991), Vol. 329, pp. 59–79.
[6] L. N. Bell, M. J. Hageman, and L. M. Muraoka, J. Pharm. Sci. **84**, 707 (1995).
[7] S. P. Duddu, G. Zang, and P. R. Dal Monte, Pharm. Res. **14**, 596 (1997).
[8] W. Wang, Int. J. Pharm. **203**, 1 (2000).
[9] M. P. Buera, S. Rossi, S. Moreno, and J. Chirife, Biotechnol. Prog. **15**, 577 (1999).
[10] P. Davidson and W. Q. Sun, Pharm. Res. **18**, 474 (2001).
[11] M. T. Cicerone, A. Tellington, L. Trost, and A. Sokolov, Bioprocess International **1**, 36 (2003).
[12] J. H. Crowe, L. M. Crowe, and D. Chapman, Science **223**, 701 (1984).
[13] B. Roser, Trends Food Sci. Technol. **2**, 166 (1991).
[14] S. D. Allison, B. Chang, T. W. Randolph, and J. F. Carpenter, Arch. Biochem. Biophys. **365**, 289 (1999).
[15] K. Tanaka, T. Takeda, and K. Miyajima, Int. J. Cardiol. **39**, 1091 (1991).
[16] J. L. Cleland, X. Lam, B. Kendrick *et al.*, J. Pharm. Sci. **90**, 310 (2001).
[17] S. Magazu, G. Maisano, H. D. Middendorf, P. Migliardo, A. M. Musolino, and M. Villari, J. Phys. Chem. B **102**, 2060 (1998).
[18] C. A. Angell, Science **267**, 1924 (1995).
[19] S. Magazu, P. Migliardo, A. M. Musolino, and M. T. Sciortino, J. Phys. Chem. B **101**, 2348 (1997).
[20] D. P. Miller, J. J. de Pablo, and H. Cort, Pharm. Res. **14**, 578 (1997).
[21] M. C. Donnamaria, E. I. Howard, and J. R. Grigera, J. Chem. Soc., Faraday Trans. **90**, 2731 (1994).
[22] Q. Liu, R. K. Schmidt, B. Teo, P. A. Karplus, and J. W. Brady, J. Am. Chem. Soc. **119**, 7851 (1997).
[23] G. Bonanno, R. Noto, and S. L. Fornilli, J. Chem. Soc., Faraday Trans. **94**, 2755 (1998).
[24] P. B. Conrad and J. J. de Pablo, J. Phys. Chem. A **103**, 4049 (1999).
[25] M. T. Cicerone and C. L. Soles, Biophys. J. **86**, 3836 (2004).
[26] A. P. Sokolov, E. Rossler, A. Kisliuk, and D. Quitmann, Phys. Rev. Lett. **71**, 2062 (1993).
[27] G. Caliskan, D. Mechtani, S. Azzam *et al.*, J. Chem. Phys. **121**, 1978 (2004).
[28] P. W. Fenimore, H. Frauenfelder, B. H. McMahon, and F. G. Parak, Proc. Natl. Acad. Sci. U.S.A. **99**, 16047 (2002).
[29] A. Paciaroni, S. Cinelli, and G. Onori, Biophys. J. **83**, 1157 (2002).
[30] J. Wang, R. M. Wolf, J. W. Caldwell, P. A. Kollman, and D. A. Case, J. Comput. Chem. **25**, 1157 (2004).
[31] D. A. Case, D. A. Pearlman, J. W. Caldwell *et al.*, AMBER7 (University of California, San Francisco, 2002).
[32] G. M. Brown, D. C. Rohrer, B. Berking, C. A. Beevers, R. O. Gould, and R. Simpson, Acta Crystallogr., Sect. B: Struct. Crystallogr. Cryst. Chem. **28**, 3145 (1972).
[33] H. van Koningsveld, Recl. Trav. Chim. Pays-Bas **87**, 243 (1968).
[34] M. J. Frisch, G. W. Trucks, H. B. Schlegel *et al.*, GAUSSIAN 03, Revision A.1 Gaussian, Inc., Pittsburgh PA, 2003.
[35] H. J. C. Berendsen, J. P. M. Postma, W. F. van Gunsteren, A. DiNola, and J. R. Haak, J. Chem. Phys. **81**, 3684 (1984).
[36] L. Xu, X. Hu, and R. Lin, J. Solution Chem. **32**, 363 (2003).
[37] J. Zang and G. Zografi, J. Pharm. Sci. **90**, 1375 (2001).
[38] M. Mezei and J. Beveridge, J. Chem. Phys. **74**, 622 (1981).
[39] R. Surana, A. Pyne, and R. Suryanarayanan, Pharm. Res. **21**, 1167 (2004).
[40] W. Humphrey, A. Dalke, and K. Schulten, J. Mol. Graphics **13**, 33 (1996).